CHEMISTRY
AN ASIAN JOURNAL

DOI: 10.1002/asia.201101049

Lamellarins as Inhibitors of P-Glycoprotein-Mediated Multidrug Resistance in a Human Colon Cancer Cell Line

Fabien Plisson, Xiao-Cong Huang, Hua Zhang, Zeinab Khalil, and Robert J. Capon*[a]

Abstract: Chemical analysis of a *Didemnum* sp. (CMB-01656) collected during scientific Scuba operations off Wasp Island, New South Wales, yielded five new lamellarins A1 (**1**), A2 (**2**), A3 (**3**), A4 (**4**) and A5 (**5**) and eight known lamellarins C (**6**), E (**7**), K (**8**), M (**9**), S (**10**), T (**11**), X (**12**) and χ (**13**). Analysis of a second *Didemnum* sp. (CMB-02127) collected during scientific trawling operations along the Northern Rottnest Shelf, Western Australia, yielded the new lamellarin A6 (**14**) and two known lamellarins G (**15**) and Z (**16**). Structures were assigned to **1**–**16** on the basis of detailed spectroscopic analysis with comparison to literature data and authentic samples. Access to this unique library of natural lamellarins (**1**–**16**) provided a rare opportunity for structure–activity relationship (SAR) investigations, probing interactions between lamellarins and the ABC transporter efflux pump P-glycoprotein (P-gp) with a view to reversing multidrug resistance in a human colon cancer cell line (SW620 Ad300). These SAR studies, which were expanded to include the permethylated lamellarin derivative (**17**) and a series of lamellarin-inspired synthetic coumarins (**19**–**24**) and isoquinolines (**25**–**26**), successfully revealed **17** as a promising new non-cytotoxic P-gp inhibitor pharmacophore.

Keywords: cancer · inhibitor · lamellarin · multidrug resistance · p-glycoprotein

Introduction

Multidrug resistance (MDR) is a major challenge to modern healthcare, seriously compromising the effectiveness of a wide variety of therapeutic agents, most notably anticancer and anti-infective drugs. ATP-binding cassette (ABC) transporters are plasma membrane proteins and an important determinant of MDR, with the human *MDR1* gene product P-glycoprotein (P-gp), also known as ABCB1 and MDR1, being the first ABC transporter to be characterized by its ability to confer MDR in cancer cells.[1] P-gp is expressed in many normal cells, including those in kidney, liver, colon, pancreas, and adrenal tissues, and in endothelial cells at the blood–brain barrier, where its broad substrate recognition and high transport capacity provide cellular protection against many endogenous and exogenous toxins. Notwithstanding its important natural role, cancers that acquire the ability to overexpress P-gp (i.e., acute myeloid leukemia, lung carcinoma, neuroblastoma, and advanced ovarian and breast carcinoma) typically correlate with poor patient prognosis.[2] This correlation is a function of P-gp utilizing ATP hydrolysis to drive transmembrane efflux of many clinically important anticancer agents, including anthracyclins (doxorubicin and daunorubicin), vinca alkaloids (vinblastine and vincristine), and taxanes (paclitaxel and docetaxel), rendering cancer cell lines overexpressing P-gp multidrug-resistant.[3] Not surprisingly, pharmaceutical inhibition of P-gp and the associated drug efflux has been viewed as an attractive strategy for combating MDR. Unfortunately, and despite much effort, clinically useful P-gp inhibitors have proved elusive. Key among the hurdles faced in bringing P-gp inhibitors to the clinic is the need to engineer for high in vivo P-gp inhibitory potency and selectivity, with low toxicity, while not adversely influencing the normal processes that regulate the safe and timely distribution and clearance of highly cytotoxic chemotherapeutic agents. Notwithstanding these concerns, should a clinically useful P-gp inhibitor be developed, the implications for cancer treatment and patient survival could be profound.

While not underestimating the scale of the challenge outlined above, we were encouraged to note that a number of natural product P-gp inhibitors (e.g., cyclosporine A and quinine) have attracted considerable attention, while also observing that other natural product-derived inhibitor structure classes have been reported but have yet to be fully explored. In the latter category our attention was drawn to the lamellarin class of marine alkaloids. First isolated in 1985 by Faulkner et al. from a Pacific Ocean marine prosobranch mollusk (*Lamellaria* sp.), several dozen lamellarins have since been reported from ascidia (*Didemnum* spp.), sponges (*Dendrilla cactos*), and mollusks (*Coriocella hibyae)* sourced from many regions (i.e., the Indian, Pacific, and Southern Oceans, and the Arabian Sea).[4] A number of lamellarins

[a] F. Plisson, X.-C. Huang, Dr. H. Zhang, Z. Khalil, Prof. R. J. Capon
Division of Chemistry and Structural Biology
Institute for Molecular Bioscience
The University of Queensland
360 Carmody Road, St Lucia, Brisbane, 4072, Queensland (Australia)
Fax: (+61) 7-334-62090
E-mail: r.capon@uq.edu.au

Supporting information for this article is available on the WWW under http://dx.doi.org/10.1002/asia.201101049.

have been reported to exhibit significant cytotoxicity, with IC_{50} values in the submicromolar range, against a range of cancer cell lines,[4–5] with a subset of lamellarins being identified as effective against P-gp–overexpressing MDR cancer cell lines.[6] With respect to MDR, Quesada et al. demonstrated in 1996 that P-gp–mediated efflux of doxorubicin, daunorubicin, and vinblastine in a murine lymphoid leukemia cell line (P388/Schabel) could be fully reversed by cotreatment with a subcytotoxic 2 μM dosage of lamellarin I (**18**).[7] The same authors alluded to other lamellarins displaying P-gp inhibitory properties (although the data were not shown),[7] and went on to patent the lamellarin class for the treatment of MDR cancers.[8] While interest in the lamellarin structure class has been sustained over the quarter century since their first discovery, with many valuable contributions from natural products, synthetic, and medicinal chemists,[4–5] these reports have not extended to a structure–activity relationship (SAR) study aimed at probing and defining molecular interactions between lamellarins and P-gp. We took the view that such an SAR analysis would advance our understanding of this unique marine pharmacophore and potentially promote the future development of lamellarin-inspired P-gp inhibitors.

Results and Discussion

As part of a marine biodiscovery program we assessed a library of about 2600 southern Australian marine invertebrates and algae for growth inhibitory activity against parental (SW620) and P-gp–overexpressing (SW620 Ad300) colon cancer cell lines. Chemical and spectroscopic profiling (HPLC–DAD–MS and ^{1}H NMR) of a particularly cytotoxic extract from a *Didemnum* sp. (CMB-01656) specimen collected during scientific Scuba operations off Wasp Island, New South Wales, revealed a complex mixture of aromatic alkaloids. This mixture was subsequently resolved by solvent extraction, partitioning and trituration, followed by reversed-phase HPLC, to yield thirteen members of the lamellarin class of marine alkaloids. These metabolites included five new examples, lamellarin A1 (**1**), lamellarin A2 (**2**), lamellarin A3 (**3**), lamellarin A4 (**4**), and lamellarin A5 (**5**), together with eight known examples, lamellarin C (**6**),[9] lamellarin E (**7**),[10] lamellarin K (**8**),[11] lamellarin M (**9**),[11] lamellarin S (**10**),[12] lamellarin T (**11**),[13] lamellarin X (**12**),[13] and lamellarin χ (**13**) (of which the latter has previously been first described as an acetylated derivative[14] and synthesized in 2006[15]). To support lamellarin structure–activity relationship investigations described later in this report, we examined a second *Didemnum* sp. (CMB-02127) sample collected during scientific trawling operations along the Northern Rottnest Shelf, Western Australia. Although not a priority hit in our screening, this extract nevertheless analyzed for a complex mixture of alkaloids that included as minor metabolites the new lamellarin A6 (**14**) together with the known lamellarin G (**15**)[10] and lamellarin Z (**16**).[16] [Note: in extending the existing lamellarin trivial nomenclature, we have elected to label the new examples of this structure class as lamellarins A1–A6.]

Table 1. Chemical structures of lamellarins **1**–**18**.

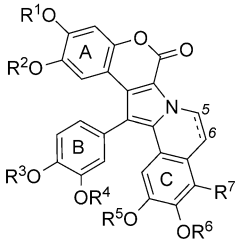

#	R^1	R^2	R^3	R^4	R^5	R^6	R^7	$\Delta^{5,6}$[a]
1	H	H	H	Me	Me	H	H	–
2	H	H	H	Me	Me	Me	OH	–
3	H	Me	H	Me	Me	Me	H	–
4	H	H	H	H	H	H	H	–
5	H	H	H	Me	H	H	H	$\Delta^{5,6}$
6	H	Me	H	Me	Me	Me	OMe	–
7	H	Me	Me	H	Me	Me	OH	–
8	H	Me	H	Me	Me	Me	OH	–
9	H	Me	H	Me	Me	Me	OH	$\Delta^{5,6}$
10	H	H	H	H	Me	H	H	–
11	H	Me	Me	H	Me	Me	OMe	–
12	H	Me	Me	H	Me	Me	OH	$\Delta^{5,6}$
13	H	Me	H	Me	Me	H	H	–
14	Me	H	H	Me	Me	H	H	-
15	Me	H	Me	H	Me	H	H	-
16	Me	H	H	H	Me	H	H	-
17	Me	Me	Me	Me	Me	Me	H	-
18	H	Me	Me	Me	Me	Me	OMe	-

[a] $\Delta^{5,6}$, unsaturated bond C-5/C-6.

Structures were assigned to lamellarins **1**–**16** (Table 1) on the basis of detailed spectroscopic analysis with comparison to literature data and authentic samples where available. The ^{13}C NMR data for **1**–**16** are summarized in Table 2, while comprehensive accounts of 1D and 2D NMR data are documented in the Supporting Information. The structure elucidation of the new lamellarins A1–A6 (**1**–**5**, **14**) and lamellarin χ (**13**) are presented below, supported by Figures 1–7 which illustrate key 2D NMR correlations.

High-resolution mass spectrometry (HRMS) data, acquired in ESI+ mode, were obtained for **1**–**5**, **13**, and **14**. The data for **1** revealed a quasi-molecular ion $(M+H)^+$ corresponding to a molecular formula $C_{27}H_{21}NO_8$, with NMR

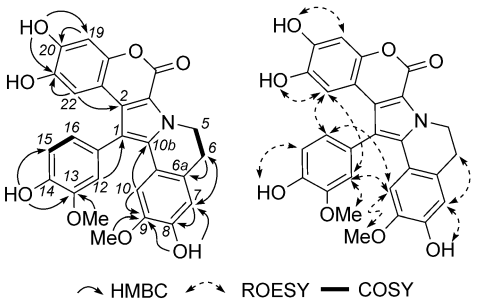

Figure 1. Key 2D NMR ([D$_6$]DMSO) correlations for lamellarin A1 (**1**).

Table 2. ^{13}C NMR ([D$_6$]DMSO) data for lamellarins **1**–**16**.[c]

#	(**1**)	(**2**)	(**3**)	(**4**)	(**5**)	(**6**)	(**7**)[a]	(**8**)[a]	(**9**)	(**10**)	(**12**)	(**13**)	(**14**)	(**15**)	(**16**)
1	114.6	115.7	114.6	114.6	n.d.	116.0	115.0	115.7	115.0	114.5	114.7	114.2	114.2	114.2	114.7
2	127.6	127.3	127.5	127.5	129.0	127.6	127.2	127.8	129.1	127.3	128.3	127.6	n.d.	126.7	126.9
3	n.d.	112.6	n.d.	112.1	n.d.	n.d.	112.5	112.9	107.1	112.3	107.3	n.d.	n.d.	112.4	112.4
5	42.0	41.7	42.0	42.0	n.d.	41.3	41.6	41.9	121.2	41.9	120.8	42.0	41.7	41.9	41.9
6	27.6	21.3	27.8	27.8	112.9	21.2	21.1	21.5	107.7	27.6	107.2	27.5	27.3	27.4	27.5
6a	127.3	114.3	126.8	125.7	124.2	120.1	114.2	114.5	112.3	127.2	111.7	127.1	127.0	127.0	127.1
7	115.3	147.2	111.8	115.0	111.8	150.3	147.2	147.6	148.9	115.2	145.5	115.3	115.0	115.2	115.2
8	147.0	136.3	148.8	146.0	147.5	141.8	136.3	136.7	133.5	146.9	135.7	146.9	146.7	146.9	147.0
9	146.1	150.7	146.8	143.5	146.6	151.2	150.7	151.1	153.0	145.9	152.6	145.9	145.8	145.8	145.9
10	109.2	100.9	108.6	113.4	109.8	104.7	100.8	101.3	97.5	109.2	97.0	109.2	108.9	109.0	109.3
10a	118.2	122.5	119.2	118.5	118.6	122.4	122.2	122.8	121.1	118.2	120.7	118.1	117.0	117.8	118.0
10b	136.2	135.4	135.5	135.9	n.d.	134.8	135.0	135.5	136.0	136.0	133.0	135.8	135.9	135.9	136.0
11	125.4	125.5	125.2	125.4	125.5	125.2	127.2	125.9	125.6	125.5	127.0	125.4	125.2	127.1	125.3
12	114.6	114.5	114.5	117.4	114.5	114.1	117.7	115.1	115.2	117.7	117.8	114.6	114.2	117.6	117.8
13	148.6	148.5	148.5	145.8	148.8	148.6	147.4	148.8	148.0	146.1	147.6	148.4	148.5	147.3	146.2
14	146.5	146.5	146.4	145.1	147.1	146.5	147.5	146.8	146.5	145.3	148.0	146.5	146.6	147.3	145.4
15	116.4	116.4	116.3	116.7	117.2	115.9	113.3	116.5	116.6	116.6	113.2	116.3	116.1	113.3	116.7
16	123.3	123.1	123.4	121.2	123.5	122.9	121.4	123.8	124.0	121.6	121.7	123.4	122.9	121.3	121.4
17	109.2	109.1	108.6	109.2	108.9	108.6	108.4	109.0	108.4	109.3	108.0	108.8	110.2	110.0	110.2
18	144.7	144.7	146.2	144.6	145.4	146.8	146.7	147.0	147.0	144.7	147.6	146.0	144.4	144.5[b]	144.6
19	103.4	103.3	103.6	103.2	103.7	103.2	103.5	103.8	103.9	103.3	103.4	103.6	100.4	100.6	100.7
20	145.9	146.0	146.7	145.9	147.1	145.7	145.5	145.9	145.9	146.0	146.3	146.6	147.7	147.7[b]	147.8
21	142.4	142.1	144.6	141.9	142.3	144.5	144.3	144.7	144.8	142.0	144.5	144.4	142.7	142.6	142.8
22	108.6	108.6	105.1	108.8	109.8	104.7	104.9	105.3	105.9	108.7	105.2	105.1	107.9	108.2	108.4
23	n.d.	154.5	n.d.	154.4	n.d.	n.d.	154.2	154.3	154.6	154.5	n.d.	n.d.	n.d.	154.2	154.3
7-OMe	–	–	–	–	–	60.5	–	–	–	–	–	–	–	–	–
8-OMe	–	60.3	55.6	–	–	60.2	60.2	60.5	60.8	–	60.3	–	–	–	–
9-OMe	54.6	54.6	54.5	–	–	54.4	54.6	54.9	54.9	54.6	54.6	54.7	54.4	54.5	54.7
13-OMe	55.8	55.9	56.0	–	55.9	55.7	–	56.3	56.2	–	–	56.0	55.7	–	–
14-OMe	–	–	–	–	–	–	56.0	–	–	–	55.8	–	–	55.6	–
20-OMe	–	–	–	–	–	–	–	–	–	–	–	–	55.6	55.7	55.8
21-OMe	–	–	55.0	–	–	54.6	55.0	55.3	55.2	–	54.6	55.0	–	–	–

n.d., resonances not detected. [a] Values obtained as a mixture. [b] Signals interchangeable. [c] Lack of material precluded measurement of ^{13}C NMR data for lamellarin T (**11**).

([D$_6$]DMSO) data suggestive of an *O*-methyl homologue of lamellarin S (**10**).[12] Assignment of NMR resonances to 9-OMe (δ_H 2.98) and 13-OMe (δ_H 3.73) moieties was supported by diagnostic 2D NMR correlations (Figure 1), and permitted structure assignment of lamellarin A1 (**1**) as indicated.

HRMS data for **2** revealed a quasi-molecular ion $(M+Na)^+$ corresponding to a molecular formula $C_{28}H_{23}NO_9$, with NMR ([D$_6$]DMSO) data suggestive of an *O*-demethyl homologue of lamellarin K (**8**).[11] Assignment of an NMR resonance to a 21-OH (δ_H 8.96) moiety was supported by diagnostic 2D NMR correlations (Figure 2), inclusive of HMBC correlations from 21-OH to C-20 (δ_C 146.0), C-21 (δ_C 142.1), and C-22 (δ_C 108.6), and a ROESY correlation to H-22 (δ_H 6.62). These considerations permitted structure assignment of lamellarin A2 (**2**) as indicated.

HRMS data for **3** revealed a quasi-molecular ion $(M+Na)^+$ corresponding to a molecular formula $C_{29}H_{25}NO_8$, with NMR ([D$_6$]DMSO) data suggestive of a deoxy analogue of lamellarin K (**8**).[11] Diagnostic 2D NMR correlations (Figure 3), inclusive of an HMBC correlation from 8-OMe (δ_H 3.77) to C-8 (δ_C 148.8), and ROESY correlation between 8-OMe and H-7 (δ_H 6.98), permitted structure assignment of lamellarin A3 (**3**) as indicated.

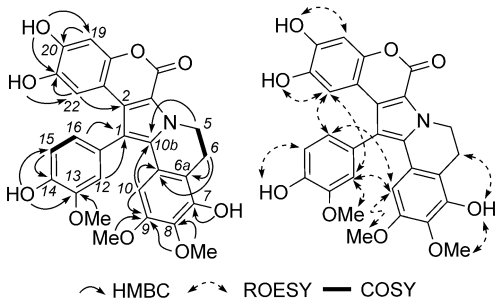

Figure 2. Key 2D NMR ([D$_6$]DMSO) correlations for lamellarin A2 (**2**).

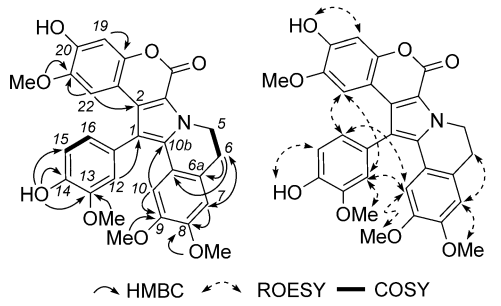

Figure 3. Key 2D NMR ([D$_6$]DMSO) correlations for lamellarin A3 (**3**).

HRMS data for **4** revealed a quasi-molecular ion $(M+H)^+$ corresponding to a molecular formula $C_{25}H_{17}NO_8$, with NMR ([D_6]DMSO) data suggestive of a dihydro analogue of lamellarin H.[10] The appearance of sp^3-hybridized ^{13}C NMR resonances for C-5 (δ_C 42.0) and C-6 (δ_C 27.8), supported by diagnostic 2D NMR correlations (Figure 4),

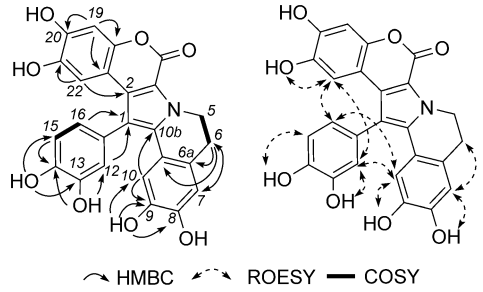

Figure 4. Key 2D NMR ([D_6]DMSO) correlations for lamellarin A4 (**4**).

permitted structure assignment of lamellarin A4 (**4**) as indicated.

HRMS data for **5** revealed a quasi-molecular ion $(M+H)^+$ corresponding to a molecular formula ($C_{26}H_{15}NO_8$) isomeric with lamellarin S (**10**), with NMR ([D_6]DMSO) data suggestive of an *O*-methyl homologue of lamellarin H.[10] Assignment of a ^1H NMR resonance for 13-OMe (δ_H 3.74) was supported by diagnostic 2D NMR correlations (Figure 5) and permitted structure assignment of la-

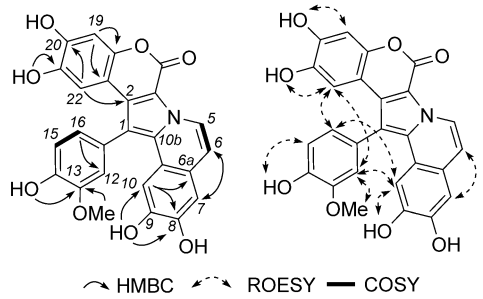

Figure 5. Key 2D NMR ([D_6]DMSO) correlations for lamellarin A5 (**5**).

mellarin A5 (**5**) as indicated.

HRMS data for **14** revealed a quasi-molecular ion $(M+H)^+$ corresponding to a molecular formula ($C_{28}H_{23}NO_8$) isomeric with lamellarins G (**15**)[10] and L,[11] with NMR ([D_6]DMSO) data suggestive of an *O*-methyl homologue of lamellarin Z (**16**).[16] Assignment of a ^1H NMR resonance for 13-OMe (δ_H 3.73) was supported by diagnostic 2D NMR correlations (Figure 6) and permitted structure assignment of lamellarin A6 (**14**) as indicated.

HRMS data for **13** revealed a quasi-molecular ion $(M+Na)^+$ corresponding to a molecular formula ($C_{28}H_{23}NO_8$) isomeric with lamellarin L with NMR ([D_6]DMSO) data suggestive of an *O*-methyl homologue of

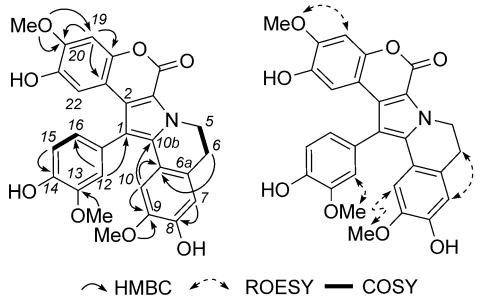

Figure 6. Key 2D NMR ([D_6]DMSO) correlations for lamellarin A6 (**14**).

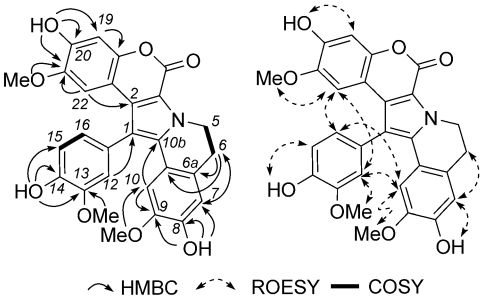

Figure 7. Key 2D NMR ([D_6]DMSO) correlations for lamellarin χ (**13**).

lamellarin A1 (**1**). Analysis of the 2D NMR data for **13** revealed diagnostic correlations (Figure 7) inclusive of an HMBC correlation from 21-OMe (δ_H 3.35) to C-21 (δ_C 144.4), and ROESY correlations between 21-OMe and H-22 (δ_H 6.60), that permitted structure assignment of lamellarin χ (**13**) as indicated.

To assess interactions between the lamellarins **1**–**16** and P-gp, we undertook a series of experiments (a summary of the results is presented in Table 3). In a primary cytotoxicity (MTT) assay, the comparative cytotoxicity of **1**–**16** was assessed against the P-gp–overexpressing human colon adenocarcinoma cell line SW620 Ad300 and the corresponding parental cell line SW620. The significantly reduced cytotoxicity against SW620 Ad300 compared to SW620 suggested that lamellarins A1 (**1**), A2 (**2**), and S (**10**) could be P-gp substrates,[17] whereas comparable levels of cytotoxicity against both cell lines suggested that lamellarins K (**8**), E (**7**), M (**9**), A3 (**3**), χ (**13**), and A6 (**14**) were not P-gp substrates. The increased cytotoxicity (≥ 4-fold) of A1 (**1**), A2 (**2**), and S (**10**) in the presence of the P-gp inhibitor cyclosporine A in SW620 Ad300 confirmed these three lamellarins as P-gp substrates. By contrast, the lack of cytotoxicity to either cell line exhibited by lamellarins A4 (**4**), A5 (**5**), C (**6**), G (**15**), and Z (**16**) left their P-gp substrate status unresolved. In a second round of screening (MDR reversal), the P-gp non-substrates **3**, **7**–**9**, and **13**–**14** were assessed for their ability to reverse P-gp–mediated doxorubicin drug resistance in the SW620 Ad300 cell line. Although all these lamellarins exhibited reversal of doxorubicin resistance, with gains in sensitivity (GS) ranging from 2.02 to 4.26, assessment of compa-

Table 3. Lamellarin interactions with P-glycoprotein.

#[a]	SW620 IC_{50} (μM)[b]	SW620 Ad300 IC_{50} (μM)[b]	IC_{50} (μM)+CsA[c]	MDR reversal GS[d]	Calcein FAR[e]
4	>30	>30	–	0.96 (20)	0.63
5	>30	>30	–	1.52 (20)	0.80
6	>30	>30	–	1.58 (20)	0.92
15	>30	>30	–	–	1.15
16	>30	>30	–	2.51 (20)	0.80
1	3.59	37.0	6.80	–	1.07
2	9.47	55.5	10.6	–	1.14
10	8.50	103	5.42	–	1.64
8	0.50	1.09	–	2.11 (0.1)	39.4
7	4.26	5.35	–	4.01 (1)	38.6
9	1.02	2.09	–	2.02 (0.5)	27.2
3	19.7	28.4	–	4.26 (5)	18.8
13	6.72	12.3	–	2.23 (3)	11.7
14	23.8	28.0	–	2.91 (10)	9.22
17	28.2	23.4	–	7.80 (3)	27.4

– = not tested. [a] Due to a lack of material, **11** and **12** were not tested. [b] Cytotoxicity (MTT) assay for lamellarins. [c] Cytotoxicity (MTT) assay for lamellarins in presence of cyclosporine A (CsA 3 μM). [d] MDR reversal (doxorubicin) assay against SW620 Ad300 where GS (gain in sensitivity) = IC_{50} of doxorubicin without lamellarin/IC_{50} of doxorubicin with lamellarin (test concentration in μM is shown in parentheses). IC_{50} of doxorubicin without lamellarin was 4.43 μM; verapamil (2.5 μM) was used as a positive control (GS = 6.23). [e] Cell flow cytometry analysis of intracellular calcein fluorescence: FAR (fluorescence arbitrary ratio) = calcein fluorescence intensity (Geo mean) in the presence of lamellarin at 20 μM/calcein fluorescence intensity (Geo mean) in the presence of PBS. Positive control is verapamil at 20 μM which returns a FAR = 43.1.

rative potency proved problematic given the need to test lamellarins at concentrations below their respective IC_{50} values (spanning 0.1 to 10 μM). To address this limitation, in a third round of screening (Calcein AM), the P-gp inhibitory activities of **3**, **7**–**9**, and **13**–**14** were assessed by brief exposure (0.5 h) of individual lamellarins (20 μM) to SW620 Ad300 cells, followed by immediate quantification of intracellular (calcein) fluorescence by cell flow cytometry. After compensating for baseline levels of intracellular fluorescence, and standardizing to the positive control verapamil (20 μM), lamellarins could be ranked as either strong (**8** and **7**), moderate (**9**), or weak (**3**, **13**, and **14**) P-gp inhibitors. On applying the MDR reversal and Calcein AM assays to the P-gp substrates, lamellarins **1**, **2**, and **10**, and the non-cytotoxic lamellarins **4**–**6** and **15**–**16**, we determined that none of these metabolites were P-gp inhibitors.

While the lamellarins **1**–**16** exhibit many common structural features, SAR analysis of our screening data (Table 3) highlighted some useful correlations. Lamellarins **1**–**16** can be grouped according to the degree of methylation, ranging across unmethylated **4**, monomethylated **5** and **10**, dimethylated **1** and **16**, trimethylated **2** and **13**–**15**, tetramethylated **3** and **7**–**9**, to pentamethylated **6** and **11**–**12**. Our SAR data suggest that the P-gp inhibitory activity loosely correlates with higher levels of methylation on rings A and B (i.e., tetramethylated **7**–**9** but not the pentamethylated **6**). The hexamethylated lamellarin I (**18**),[7] the only lamellarin with published data supportive of P-gp inhibitory activity, is consistent with this methylation hypothesis. Building on this emerging SAR, we permethylated lamellarin S to lamellarin derivative **17** to test the hypothesis that further increasing lamellarin methylation would enhance P-gp inhibitory activity. In addition, we assembled a selection of lamellarin-inspired synthetic coumarins (**19**–**24**) and isoquinolines (**25**–**26**) to test the hypothesis that lamellarin P-gp inhibitory activity is inherent to embedded structure fragments. Subsequent assays established that, whereas the lamellarin-inspired coumarin and isoquinoline fragments **19**–**26** (Figure 8) did not exhibit P-gp inhibitory activity, the hexamethylated lamellarin **17**, obtained by K_2CO_3/MeI treatment, was a potent P-gp inhibitor (fluorescence arbitrary ratio FAR of 27.4) and a very strong MDR reversal agent (GS of 7.80 at 3 μM). Also of note, **17** was less cytotoxic towards either colon cancer cell line (Table 3). While these results support our initial hypothesis regarding a correlation between methylation and P-gp inhibition, they also suggest that the molecular basis behind lamellarin P-gp inhibitory activity requires the intact molecular architecture of the natural product scaffold.

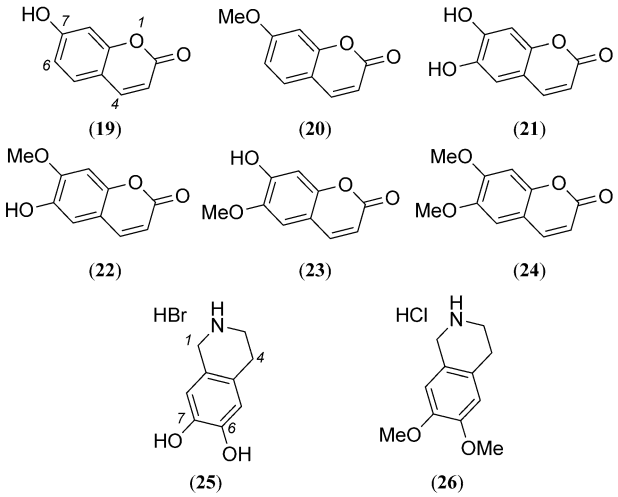

(19) (20) (21) (22) (23) (24) (25) (26)

Figure 8. Lamellarin-inspired synthetic coumarins (**19**–**24**) and isoquinolines scaffolds (**25**–**26**).

In an effort to document their broader biological profile, particularly against indications and biological targets already associated with lamellarins in the literature, the *Didemnum* lamellarins **1**–**16** were screened for antibiotic and kinase inhibitory activities. Lamellarins **1**–**16** displayed no significant growth inhibitory activity (MIC > 30 μM) against the fungus *Candida albicans* (ATCC 90028), the Gram-negative bacte-

ria *Escherichia coli* (ATCC 11775) and *Pseudomonas aeruginosa* (ATCC 10145), or the Gram-positive bacteria *Staphylococcus aureus* (ATCC 9144 and ATCC 25923) and *Bacillus subtilis* (ATCC 6051). When **1–16** were tested against *Bacillus subtilis* (ATCC 6633), only lamellarins E (**7**), K (**8**), and M (**9**) displayed antibacterial activity (MIC = 7.5, 15, and 7.5 μM respectively). When assessed against the neurodegenerative disease targets casein kinase 1 (CK1δ) and cyclin-dependent kinase 5 (CDK5), **1–16** exhibited limited inhibitory activity against CK1δ, with lamellarins A4 (**4**) and S (**10**) being the most active (IC_{50} = 3 μM). On the other hand, **1–16** displayed generally higher levels of inhibition against CDK5, with lamellarins A1 (**1**), A6 (**14**), and Z (**16**) all displaying submicromolar inhibition (0.1, 0.3, and 0.4 μM, respectively).

Conclusions

This study reports the isolation and identification of a selection of new (**1–5, 14**) and known (**6–13**, **15**, **16**) lamellarins from two southern Australian *Didemnum* sp., supported by comprehensive spectroscopic analysis. Access to a privileged library of natural lamellarins enabled SAR studies aimed at understanding interactions between this unique family of marine alkaloids and the ABC transporter efflux pump P-glycoprotein, a key determinant in MDR cancers. These studies determined that 1) the non-cytotoxic lamellarins **4–6** and **15–16** had no demonstrable interaction with P-gp, 2) the cytotoxic lamellarins **1–2** and **10** were P-gp substrates, and 3) the cytotoxic lamellarins **3, 7–9**, and **13–14** were P-gp inhibitors capable of reversing MDR. An SAR analysis of these data suggested that P-gp inhibitory activity correlated with higher levels of lamellarin methylation, a hypothesis that was tested and supported by synthesis and evaluation of the permethylated lamellarin **17**. Significantly, not only did **17** exhibit strong MDR reversal and potent inhibition of P-gp but these enhancements also coincided with a significant reduction in cytotoxicity. By contrast, efforts to attribute the lamellarin P-gp inhibitory activity to the simpler synthetic structure fragments **19–26** failed, reinforcing the importance of discovery through the screening of highly evolved intact natural product scaffolds.

The observations made above draw attention to the possible ecological value of maintaining a combinatorial cohort of differentially methylated lamellarin co-metabolites, which at first glance may seem a biosynthetic extravagance on behalf of the *Didemnum* sp. In an ecological setting the suite of lamellarin co-metabolites could be viewed as potentially far more valuable to the *Didemnum* sp. than any individual lamellarin, irrespective of relative cytotoxicity. For example, by a modest biosynthetic investment (methyl transferase) the *Didemnum* sp. can deploy more highly methylated lamellarins (as P-gp inhibitors) to potentiate the ecological impact of less methylated lamellarins (cytotoxins) when encountering competing or threatening organisms/cells equipped with P-gp–mediated cellular defences. This potentiating concept is a salutatory lesson to those who value and/or devalue natural products merely on the basis of cytotoxicity. Our investigation into *Didemnum* lamellarins reaffirms the view that non-cytotoxic natural products can exhibit valuable biological properties that allude to both an ecological advantage and a pharmacological potential.

Experimental Section

General Experimentals

General procedures, instrumentation, HPLC chromatograms, characterization data, and screening and assay results are presented in the Supporting Information.

Collection and Taxonomy

Sample CMB-01656 was collected by Scuba diving in July 1994 off Wasp Island Durras NSW (35°40.1′S, 150°18.5′E) at a depth of 15–20 m. Sample CMB-02127 was collected in January 1996 by using an epibenthic sled off the northern Rottnest Shelf, Western Australia. Freshly collected samples were frozen (−4 °C) for shipping to the laboratory, where they were thawed, catalogued, subjected to taxonomic classification as *Didemnum* sp., diced, and steeped in aqueous EtOH at −30 °C for prolonged storage.

Extraction and Isolation

A portion of the aqueous EtOH extract of sample CMB-01656 was decanted and concentrated in vacuo, and the residue (737.9 mg) partitioned between H_2O and *n*BuOH. The *n*BuOH-soluble fraction was concentrated in vacuo (108.9 mg) and the residue further triturated into light petroleum (21.6 mg), CH_2Cl_2 (27.5 mg), MeOH (55.8 mg), and H_2O (665.5 mg) solubles. The CH_2Cl_2 solubles were subjected to HPLC fractionation (Agilent Zorbax Eclipse 5 μm, 250 × 9.4 mm column, 4 mL min^{-1} gradient elution, 90% H_2O/MeCN to 100% MeCN with a constant 0.01% TFA/MeCN modifier over 20 min) to yield eight fractions. Fractions 2–5 yielded lamellarins S (**1**) (1.4 mg, 0.051%), A1 (**1**) (1.3 mg, 0.012%), A2 (**2**) (1.5 mg, 0.014%), and χ (**13**) (1.5 mg, 0.014%), respectively. Fraction 6 was a mixture (32:35:22:11) of lamellarins E (**7**) (1.6 mg, 0.015%), K (**8**) (2.0 mg, 0.018%), M (**9**) (0.6 mg, 0.005%), and X (**12**) (0.3 mg, 0.003%). Fraction 7 was pure lamellarin A3 (**3**) (0.9 mg, 0.008%). HPLC resolution of fraction 8 (1.3 mg) (Agilent Zorbax SB C_3 5 μm, 150 × 4.6 mm column, first with a 1 mL min^{-1} gradient elution, 75% H_2O/MeOH to 100% MeOH with a constant 0.01% TFA/MeOH modifier over 15 min, followed by a 1 mL min^{-1} isocratic elution 100% MeOH with a constant 0.01% TFA/MeOH modifier over 3 min), afforded lamellarins T (**11**) (0.2 mg, 0.002%) and C (**6**) (0.3 mg, 0.003%). The MeOH solubles were subjected to HPLC fractionation (Agilent Zorbax Eclipse C_{18} 5 μm, 250 × 9.4 mm column, 4 mL min^{-1} gradient elution, 90% H_2O/MeOH to 100% MeOH with a constant 0.01% TFA/MeOH modifier over 20 min) to yield nine fractions. Fractions 3 and 5–8 yielded lamellarins A4 (**4**) (1.3 mg, 0.012%), S (**10**) (17.9 mg, 0.164%), A5 (**5**) (1.1 mg, 0.010%), A1 (**1**) (1.7 mg, 0.016%), and A2 (**2**) (3.2 mg, 0.029%), respectively. HPLC resolution of fraction 9 (2.2 mg) (Agilent Zorbax SB C_{18} 5 μm, 150 × 4.6 mm column, first with a 1 mL min^{-1} gradient elution, 90% H_2O/MeCN to 40% H_2O/MeCN with a constant 0.01% TFA/MeCN modifier over 18 min, followed by a 1 mL min^{-1} gradient elution 40% H_2O/MeCN to 100% MeCN with a constant 0.01% TFA/MeCN modifier over 2 min), afforded lamellarins K (**8**) (0.5 mg, 0.005%) and E (**7**) (0.5 mg, 0.005%).

A portion of the aqueous EtOH extract of sample CMB-02127 was decanted and concentrated in vacuo, and the residue (869.8 mg) partitioned between H_2O and *n*BuOH. The *n*BuOH-soluble fraction was concentrated in vacuo (153.8 mg) and the residue further triturated into light petroleum (5.7 mg), CH_2Cl_2 (9.7 mg), MeOH (129.2 mg), and water (649.1 mg) solubles. The MeOH solubles were subjected to HPLC fractionation (Agilent Zorbax Eclipse 5 μm, 250 × 9.4 mm column, 4 mL min^{-1} gradient

elution, 90% H_2O/MeCN to 100% MeCN with a constant 0.01% TFA/MeCN modifier over 22 min) to yield fourteen fractions. Fraction 13 was pure lamellarin Z (**16**) (0.3 mg, 0.002%). HPLC resolution of fraction 14 (4.2 mg) (Agilent Zorbax SB C_3 5 μm, 150×4.6 mm column, first with a 1 mL min^{-1} gradient elution, 90% H_2O/MeCN to 30% H_2O/MeCN with a constant 0.01% TFA/MeCN modifier over 18 min, followed by a 1 mL min^{-1} gradient elution 30% H_2O/MeOH to 100% MeOH with a constant 0.01% TFA/MeOH modifier over 7 min), afforded lamellarin G (**15**) (0.3 mg, 0.002%) and A6 (**14**) (0.5 mg, 0.003%).

[Note: % yields are expressed as a mass-to-mass % compared to the weight of the *n*BuOH solubles].

Cell Lines and Cell Culture

The parental cell line SW620 (American Type Culture Collection, Manassasm VA, CCL-227), is a human colon cell line that originated from a lymph node metastasis in a patient with primary adenocarcinoma of the colon. The multidrug-resistant (MDR) cell line SW620 Ad300, which overexpresses P-gp, was selected from SW620 by growth in the presence of increasing concentrations of doxorubicin. SW620 and SW620 Ad300 cells were grown in flasks as adherent monolayers in RPMI medium supplemented with 10% fetal bovine serum, 2 mM L-glutamine, 100 units mL^{-1} penicillin and 100 μg mL^{-1} streptomycin in a humidified incubator under 5% CO_2 at 37 °C. After SW620 Ad300 exhibited stable phenotype of P-gp, the cells were maintained in 300 ng mL^{-1} doxorubicin.

Cytotoxicity (MTT) Assay

The cytotoxicity MTT assay was used to evaluate the cytotoxicity of compounds against cancer cells. This assay was modified slightly from that previously described.[18] Briefly, cells (2000 per well in 180 μL of RPMI 1640 supplemented with 10% FBS) were seeded evenly in a 96-well microplate, and the plate was incubated for 18 h at 37 °C under 5% CO_2 to allow cells to attach. Compounds to be tested were dissolved in 5% DMSO (v/v) and diluted in a range from 300 μM to300 nM. Aliquots (20 μL) of each dilution (or of 5% aqueous DMSO for control wells) were added to each well in duplicate. To evaluate the cytotoxicity of **1**, **2**, or **10** in the presence of cyclosporine A in SW620 Ad300, 2000 cells in 160 μL medium were plated onto each well. Following incubation for 18 h, increasing doses of these three lamellarins were added in the presence of 3 μM cyclosporine A. After 68 h incubation (37 °C; 5% CO_2), a solution of 3-(4,5-dimethylthiazol-2-yl)-2,5-diphenyltetrazolium bromide (MTT; Sigma, USA) in PBS was added to each well to a final concentration of 0.4 mg mL^{-1}, and the plate was incubated for a further 4 h (37 °C; 5% CO_2). After that the medium was carefully aspirated and precipitated formazan crystals were dissolved in DMSO (100 μL per well). Finally, the absorbance of each well at 580 nm was measured with a PowerWave XS Microplate Reader from Bio-Tek Instruments Inc. (Vinooski, VT). The IC_{50} value was calculated as the concentration of the compound required for 50% inhibition of the cancer cells using Prism 5.0 from GraphPad Software Inc. (La Jolla, CA).

MDR Reversal (Doxorubicin) Assay

This assay is similar to the above cytotoxicity (MTT) assay. Instead of measuring the cytotoxicity of lamellarins, this assay was applied to measure the cytotoxicity of doxorubicin against SW620 Ad300, in the presence or absence of lamellarin at concentrations that were non-cytotoxic to SW620 Ad300. Gain in sensitivity (GS) was calculated according to GS = IC_{50} of doxorubicin without lamellarin/IC_{50} of doxorubicin with lamellarin (test concentration in μM is shown in parentheses). The IC_{50} value of doxorubicin without lamellarin was 4.43 μM, 2.5 μM verapamil was used as a positive control (GS = 6.23).

Flow Cytometry (Calcein AM Assay)

The flow cytometry assay was based on that described previously.[19] Cells which overexpress P-gp (SW620 Ad300) were harvested with trypsin, resuspended in completed medium to give a final concentration of 50× 10^4 cells mL^{-1}, and pre-incubated with 20 μM lamellarin or verapamil for 30 min at 37 °C under 5% CO_2. Subsequently, cells were incubated with 2.5 μM calcein AM for 1 h followed by washing twice with cold PBS. Samples were then analyzed on a BD FACSCantoTM II flow cytometer (Becton Dickinson, San Jose, CA). Calcein fluorescence was detected with a 488 nm argon laser and a 530 nm band pass filter. The data were analyzed by using FCSexpress 3 (De Novo Software, Los Angeles, CA). 10000 events were collected for each sample. Inhibition was evaluated using the following equation: FAR (fluorescence arbitrary ratio) = calcein fluorescence intensity (Geo mean) in the presence of lamellarin at 20 μM/calcein fluorescence intensity (Geo mean) in the presence of PBS. Verapamil at 20 μM was used as a positive control (FAR = 43.1).

Antibacterial Assay

The bacterium to be tested was streaked onto a tryptic soy agar plate and was incubated at 37 °C for 24 h. One colony was then transferred to fresh tryptic soy broth (15 mL) and the cell density was adjusted to 10^4–10^5 cfu mL^{-1}. Test compounds were dissolved in DMSO and diluted with H_2O to give a 300 μM stock solution (10% DMSO). The stock solution was then serially diluted with 10% DMSO to give final concentrations of 30 μM to 0.01 μM in 1% DMSO. An aliquot (20 μL) of each dilution was transferred to a 96-well microtiter plate and freshly prepared microbial broth (180 μL) was added to each well. The plates were incubated at 37 °C for 24 h and the optical density of each well was measured spectrophotometrically at 600 nm. Each test compound was screened against the Gram-negative bacterium *Escherichia coli* (ATCC 11775) and the Gram-positive bacteria *Staphylococcus aureus* (ATCC 9144 and ATCC 25923) and *Bacillus subtilis* (ATCC 6633 and ATCC 6051).

Antifungal Assay

The fungus to be tested was streaked onto a Sabouraud agar plate and was incubated at 26.5 °C for 48 h. One colony was then transferred to fresh Sabouraud broth (15 mL) and the cell density was adjusted to 10^4–10^5 cfu mL^{-1}. Test compounds were dissolved in DMSO and diluted with H_2O to give a 300 μM stock solution (10% DMSO). The stock solution was then serially diluted with 10% DMSO to give final concentrations of 30 μM to 0.01 μM in 1% DMSO. An aliquot (20 μL) of each dilution was transferred to a 96-well microtiter plate and freshly prepared microbial broth (180 μL) was added to each well. The plates were incubated at 26.5 °C for 48 h and the optical density of each well was measured spectrophotometrically at 600 nm. Each test compound was screened against the fungus *Candida albicans* (ATCC 90028).

Kinase (CDK5) Inhibitor Assay

Test compounds (1% DMSO) were added in duplicate to a 384-well plate at desired concentrations. CDK5/p25 (0.8 ng μL^{-1}) was dispensed into wells and the plate incubated for 10 min at rt. Following addition of ATP (4 μM) and histone (300 μg mL^{-1}) to a final assay volume of 25 μL, the plate was covered with parafilm and incubated at 27 °C for 60 min. After equilibrating to rt, 20 μL of Kinase-Glo reagent was added to each well and the plate incubated for a further 10 min before luminescence was measured using a Polarstar plate reader. Concentrations given are for final assay conditions. Controls included a 'no kinase' control (ATP, histone only), 'kinase' control (CDK5/p25, ATP and histone), and a 'vehicle' control (CDK5/p25, ATP, histone and DMSO). Percent inhibition = ((test sample-kinase control)/(no kinase control-kinase control))×100. IC_{50} values were calculated using Prism. The assay buffer consisted of 6.25 mM MOPS (pH 7.2), 6.25 mM $MgCl_2$, 1.25 mM EGTA, 1.25 mM EDTA, and 0.25% glycerol. Assay components were obtained as follows: CDK5/p25 (Sigma Aldrich, C0745), ATP (Sigma Aldrich, A7699), histone (Sigma Aldrich, H4524), Kinase-Glo reagent (Promega, V6712), 384-well plates (Perkin–Elmer, 6007290).

Kinase (CK1δ) Inhibitor Assay

Test compounds (1% DMSO) were added in duplicate to a 384-well plate at desired concentrations. CK1δ (0.4 ng μL^{-1}) was dispensed into wells and the plate incubated for 10 min at rt. ATP (6 μM) and CK1tide (125 μM) were added to a final assay volume of 25 μL. The method then proceeded as described above for the kinase (CDK5) inhibitor assay. Concentrations given are for final assay conditions. Controls included a 'no kinase' control (ATP, CK1tide only), 'kinase' control (CK1δ, ATP

and CK1tide), and a 'vehicle' control (CK1δ, ATP, CK1tide, and DMSO). Percent inhibition = ((test sample−kinase control)/(no kinase control−kinase control)) × 100. IC_{50} values were calculated using Prism. The assay buffer consisted of 7.5 mM MOPS (pH 7.0), 0.25 mM EDTA, 0.003% Brij-35, 1% glycerol, 0.03% BME, 0.5 mg mL^{-1} BSA, and 12.5 mM $Mg(OAc)_2$. Assay components were obtained as described above or as follows: CK1δ (Millipore, 14–520) and Ck1tide (Millipore, 12–529).

Characterization Data for Lamellarins A1–A6 and χ

Lamellarin A1 (**1**). A pale brown oil. UV (EtOH) λ_{max} (log ε) 207 (4.64), 277 (4.34), 315 (4.28), 340 (4.27), 392 (3.54) nm; NMR ([D_6]DMSO, 600 MHz) data, see Table 2 and the Supporting Information; ESI(+)MS *m/z* 488 $[M+H]^+$; ESI(−)MS *m/z* 486 $[M-H]^-$; HRESI(+)MS *m/z* calcd for $C_{27}H_{22}NO_8$: 488.1340 $[M+H]^+$; found, 488.1340 $[M+H]^+$.

Lamellarin A2 (**2**). A brown oil. UV (EtOH) λ_{max} (log ε) 207 (4.62), 278 (4.33), 315 (4.26), 340 (4.24) nm; NMR ([D_6]DMSO, 600 MHz) data, see Table 2 and the Supporting Information; ESI(+)MS *m/z* 540 $[M+Na]^+$; ESI(+)MS *m/z* 540 $[M+Na]^+$; ESI(−)MS *m/z* 516 $[M-H]^-$; HRESI(+)MS *m/z* calcd for $C_{28}H_{23}NO_9Na$ $[M+Na]^+$: 540.1265; found: 540.1257.

Lamellarin A3 (**3**). A pale yellow oil. UV (EtOH) λ_{max} (log ε) 207 (4.60), 277 (4.32), 315 (4.24), 340 (4.20) nm; NMR ([D_6]DMSO, 600 MHz) data, see Table 2 and the Supporting Information; ESI(+)MS *m/z* 538 $[M+Na]^+$; ESI(−)MS *m/z* 514 $[M-H]^-$; HRESI(+)MS *m/z* calcd for $C_{29}H_{25}NO_8Na$ $[M+Na]^+$: 538.1472; found: 538.1469.

Lamellarin A4 (**4**). A pale green oil. UV (EtOH) λ_{max} (log ε) 208 (4.64), 276 (4.37), 315 (4.20), 337 (4.16), 392 (3.76) nm; NMR ([D_6]DMSO, 600 MHz) data, see Table 2 and the Supporting Information; ESI(+)MS *m/z* 460 $[M+H]^+$ and *m/z* 482 $[M+Na]^+$; ESI(−)MS *m/z* 458 $[M-H]^-$; HRESI(+)MS *m/z* calcd for $C_{25}H_{18}NO_8$ $[M+H]^+$: 460.1027; found: 460.1024.

Lamellarin A5 (**5**). A pale yellow oil. UV (EtOH) λ_{max} (log ε) 207 (4.67), 281 (4.38), 308 (4.22), 368 (3.90), 391 (3.97) nm; NMR ([D_6]DMSO, 600 MHz) data, see Table 2 and the Supporting Information; ESI(+)MS *m/z* 472 $[M+H]^+$; ESI(−)MS *m/z* 470 $[M-H]^-$ and *m/z* 941 $[2M-H]^-$; HRESI(−)MS *m/z* calcd for $C_{26}H_{16}NO_8$ $[M-H]^-$: 470.0890; found: 470.0881.

Lamellarin A6 (**14**). A pale yellow oil. UV (MeOH) λ_{max} (log ε) 203 (4.73), 276 (4.27), 315 (4.17), 340 (4.13) nm; NMR ([D_6]DMSO, 600 MHz) data, see Table 2 and the Supporting Information; ESI(+)MS *m/z* 502 $[M+H]^+$; ESI(−)MS *m/z* 500 $[M-H]^-$; HRESI(+)MS *m/z* calcd for $C_{28}H_{24}NO_8$ $[M+H]^+$: 502.1496; found: 502.1503.

Lamellarin χ (**13**). A colorless oil. UV (EtOH) λ_{max} (log ε) 207 (4.64), 278 (4.35), 313 (4.28), 335 (4.24) nm; NMR ([D_6]DMSO, 600 MHz) data, see Table 2 and the Supporting Information; ESI(+)MS *m/z* 524 $[M+Na]^+$; ESI(−)MS *m/z* 500 $[M-H]^-$; HRESI(+)MS *m/z* calcd for $C_{28}H_{23}NO_8Na$ $[M+Na]^+$: 524.1316; found: 524.1319.

Acknowledgements

The authors thank the CSIRO Division of Oceanography and crew of the RV Franklin for the collection of *Didemnum* sp. (CMB-02127), S. Bates and R. Robey (NCI) for providing the SW620 and SW620 Ad300 cell lines, and A. M. Piggott (IMB, UQ) for the acquisition of HRESIMS data. X.-C. Huang and Z. Khalil acknowledge the provision of International Postgraduate Scholarships from The University of Queensland. F. Plisson acknowledges the provision of an IMB Postgraduate Award. This work was partially funded by the Institute for Molecular Bioscience, The University of Queensland, the Australian Research Council (ARC LP0775547), and Noscira (Madrid, Spain).

[1] H. Glavinas, P. Krajcsi, J. Cserepes, B. Sarkadi, *Curr. Drug Delivery* **2004**, *1*, 27–42.
[2] C. Barthomeuf, M. L. Bourguet-Kondracki, J. M. Kornprobst, *Anti-cancer Agents Med. Chem.* **2008**, *8*, 886–903.
[3] N. Aouali, L. Eddabra, J. Macadre, H. Morjani, *Crit. Rev. Oncol. Hematol.* **2005**, *56*, 61–70.
[4] H. Fan, J. Peng, M. T. Hamann, J.-F. Hu, *Chem. Rev.* **2008**, *108*, 264–287.
[5] J. Kluza, P. Marchetti, C. Bailly, in *Modern Alkaloids: Structure, Isolation, Synthesis and Biology* (Eds.: E. Fattorusso, O. Taglialatela-Scafati), Wiley-VCH, Weinheim, **2008**, pp. 171–187.
[6] M. Vanhuyse, J. Kluza, C. Tardy, G. Otero, C. Cuevas, C. Bailly, A. Lansiaux, *Cancer Lett.* **2005**, *221*, 165–175.
[7] A. R. Quesada, M. D. Garcia Gravalos, J. L. Fernandez Puentes, *Br. J. Cancer* **1996**, *74*, 677–682.
[8] J. L. F. Puentes, D. Garcia Gravalos, A. R. Quesada, **1997**, *WO 9701336 (A1)*.
[9] R. J. Andersen, D. J. Faulkner, C.-H. He, G. D. V. Duyne, J. Clardy, *J. Am. Chem. Soc.* **1985**, *107*, 5492–5495.
[10] N. Lindquist, W. Fenical, G. D. V. Duyne, J. Clardy, *J. Org. Chem.* **1988**, *53*, 4570–4574.
[11] A. R. Carroll, B. F. Bowden, J. C. Coll, *Aust. J. Chem.* **1993**, *46*, 489–501.
[12] S. Urban, R. J. Capon, *Aust. J. Chem.* **1996**, *49*, 711–713.
[13] M. V. R. Reddy, D. J. Faulkner, Y. Venkateswarlu, M. R. Rao, *Tetrahedron* **1997**, *53*, 3457–3466.
[14] S. M. Reddy, M. Srinivasulu, N. Satyanarayana, A. K. Kondapi, Y. Venkateswarlu, *Tetrahedron* **2005**, *61*, 9242–9247.
[15] P. Ploypradith, T. Petchmanee, P. Sahakitpichan, N. D. Litvinas, S. Ruchirawat, *J. Org. Chem.* **2006**, *71*, 9440–9448.
[16] R. A. Davis, A. R. Carroll, G. K. Pierens, R. J. Quinn, *J. Nat. Prod.* **1999**, *62*, 419–424.
[17] S. Scala, N. Akhmed, U. S. Rao, K. Paull, L. B. Lan, B. Dickstein, J. S. Lee, G. H. Elgemeie, W. D. Stein, S. E. Bates, *Mol. Pharmacol.* **1997**, *51*, 1024–1033.
[18] C. J. Henrich, H. R. Bokesch, M. Dean, S. E. Bates, R. W. Robey, E. I. Goncharova, J. A. Wilson, J. B. McMahon, *J. Biomol. Screening* **2006**, *11*, 176–183.
[19] C. J. Henrich, R. W. Robey, K. Takada, H. R. Bokesch, S. E. Bates, S. Shukla, S. V. Ambudkar, J. B. McMahon, K. R. Gustafson, *ACS Chem. Biol.* **2009**, *4*, 637–647.

Received: December 24, 2011
Revised: February 14, 2012
Published online: ■■ ■■, 0000

FULL PAPERS

New promise in fighting MDR: This study reports a selection of new (**1**–**5**, **14**) and known (**6**–**13**, **15**–**16**) lamellarins from two southern Australian *Didemnum* sp. All structures were assigned by detailed spectroscopic analysis. This unique library of marine alkaloids, supported by semi-synthetic (**17**) and synthetic analogues (**19**–**26**), was used to probe interactions with the ABC transporter efflux pump P-glycoprotein (P-gp), leading to the discovery an optimized P-gp inhibitor capable of reversing multidrug resistance (MDR) in a human cancer cell line.

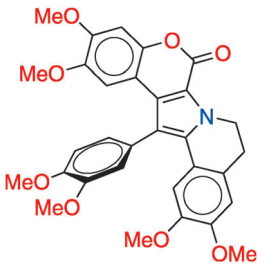

Protein Inhibitors

*Fabien Plisson, Xiao-Cong Huang, Hua Zhang, Zeinab Khalil, Robert J. Capon** ———— ▮▮▮▮–▮▮▮▮

Lamellarins as Inhibitors of P-Glycoprotein-Mediated Multidrug Resistance in a Human Colon Cancer Cell Line